Fe-Ni Alloy Synthesis Based on Nitrates Thermal Decomposition Followed by H_2 Reduction

ORFELINDA AVALO CORTEZ, FRANCISCO JOSÉ MOURA, EDUARDO DE ALBUQUERQUE BROCCHI, ROGÉRIO NAVARRO CORREIA DE SIQUEIRA, and RODRIGO FERNANDES MAGALHÃES DE SOUZA

Iron-nickel alloys have been synthesized through thermal decomposition of nitrates aqueous solutions followed by H_2 reduction. The effect of temperature [773 K to 973 K (500 °C to 700 °C)] over the oxide reduction kinetics has been studied. The results indicate that at 973 K (700 °C) and for a reaction time of 90 minutes, it was possible to obtain Fe-Ni alloys with distinct compositions. The X-ray diffraction analysis (XRD) of the initial oxide mixture has shown distinct peaks of iron and nickel oxides (Fe_2O_3, NiO, and Fe_2NiO_4). The same analysis for the reduced samples suggests that alloying has taken place. Indeed, the Rietveld analysis of the XRD patterns indicates the presence of two solid solutions—alpha (BCC) and $FeNi_3$ (FCC), with varying mass percent depending on the initial Fe to Ni ratio, in accordance with the information contained in the Fe-Ni phase diagram. The calculated alloy average crystallite size has shown to be equal to 26 nm. Total magnetization measurements suggest a superparamagnetic behavior, which is a typical result for magnetic materials of considerable nanostructured content, in accordance with the expectation based on the quantitative evaluation of the XRD data.

DOI: 10.1007/s11663-014-0221-x

I. INTRODUCTION

In general, many material properties are dependent on the particle size and, therefore, can be enhanced through its reduction to the nanometer range. Magnetic properties, for example, are positively affected by a size reduction,[1] as nanostructured particles are known to behave superparamagnetically.[2] In fact, this means that almost no hysteresis can be detected during the inversion of the applied field. As a result, the fast changing of the magnetic dipole orientations so as to get aligned with the external field can be explored for the construction of electronic devices, such as those based on magnetic random access memory technology.[3] This characteristic is potentially present in all materials, which contain magnetic elements, for example, Fe-Ni alloys, which are attractive, not only because of the associated low thermal expansion coefficient, but also for the construction of soft magnet devices.[4,5]

This particular scenario has encouraged further investigations on alternative nanostructured alloys synthesis methods. With time, chemical methods,[5–9] in comparison to the ones based on the physical mixture of pure metals followed by sintering,[10–12] achieved considerable importance, as they can easily lead to the formation of alloys of considerable nanostructured content. In relation to the physical routes, the production of pure metal nanostructured particles through milling is extensively energy dependent, and also involves significant concerns regarding the homogeneity of the samples.

Recently, our research group has worked on a two-step synthesis method based on the nitrates solution thermal decomposition followed by hydrogen reduction of the co-formed oxides,[13–15] which can easily result in nanostructured crystals of varying nature—alloys, CERMET composites, and spinels. This process has been employed in the present article for the synthesis of Fe-Ni alloys with distinct iron mole fractions. All materials, including the obtained alloys, have been characterized through quantitative X-ray diffraction analysis (XRD). Moreover, specific magnetization measurements under varying external field have been conducted for the alloy samples at 298 K (25 °C) so as to investigate the amount of magnetic hysteresis present.

II. THERMODYNAMIC BACKGROUND

The following section focuses on the thermodynamic aspects of the nitrates thermal decomposition as well as the hydrogen reduction of the resulting oxides.

ORFELINDA AVALO CORTEZ, Professor, is with the Facultad de Ingeniería Geológica, Minera y Metalúrgica - Escuela de Metalurgia (FIGMM), Universidad Nacional de Ingenieria, Av. Túpac Amaru, 210, Rimac District, Lima 25, Lima, Lima Province, Peru. FRANCISCO JOSÉ MOURA, ROGÉRIO NAVARRO CORREIA DE SIQUEIRA, and EDUARDO DE ALBUQUERQUE BROCCHI, Professors, and RODRIGO FERNANDES MAGALHÃES DE SOUZA, DSc Student, are with the Department of Materials Engineering, Pontifical Catholic University of Rio de Janeiro (DEMa/PUC-Rio), Rua Marquês de São Vicente, 225, Gávea, 22453-900 Rio de Janeiro, Rio de Janeiro, Brazil.

Manuscript submitted February 4, 2014.
Article published online October 30, 2014.

A. *Nitrates Thermal Decomposition*

Thermal decomposition of nitrates is a possible method to produce nanostructured oxide mixtures. Considering an initial mixture composed of hydrated nickel and iron nitrates, for example, through proper heating, reactions as those represented by Eqs. [1] and [2] settle in, resulting in iron and nickel oxide crystals in a homogeneous mixture state.

$$Ni(NO_3)_2 \cdot 6H_2O \leftrightarrow NiO + 2NO_2(g) + 0.5O_2(g) + 6H_2O(g), \quad [1]$$

$$2Fe(NO_3)_3 \cdot 9H_2O \leftrightarrow Fe_2O_3 + 6NO_2(g) + 1.5O_2(g) + 18H_2O(g). \quad [2]$$

The feasibility of the mentioned decomposition reactions can be appreciated by the change of standard molar Gibbs free energy, as illustrated in Figure 1. The significant negative Gibbs energy values found for temperatures higher than 523 K (250 °C) indicate that the decomposition process is thermodynamically supported at these conditions. However, if the dissociation is conducted in open systems, the continuous gaseous products removal shifts the chemical equilibrium in the desired direction, which results in significant driving force, even at lower temperatures.

B. *Hydrogen Reduction*

The thermodynamic viability of reducing iron and nickel oxides with hydrogen can be studied by the computation of the H_2 equilibrium mole fraction as function of temperature (Figure 2).

It can be noticed that even at very low partial pressures of H_2 the reduction of nickel oxide is thermodynamically favorable in the range between 673 K and 1273 K (400 °C and 1546 °C). The same is true for Fe_2O_3. However, the reduction of lower iron oxides follows different paths depending on the temperature imposed. Starting from Fe_2O_3, for temperatures below 823 K (550 °C), the first oxide formed (Fe_3O_4) should be directly reduced to iron, while for higher temperatures, the formation of FeO develops prior to the metal production. Considering the Fe_2O_3 reduction, the negligible H_2 partial pressure values suggest that this reaction is associated with a significant thermodynamic driving force. In relation to the reduction of the other possible iron oxides, it is clear that an atmosphere with a H_2 concentration higher than 80 pct should result in a full conversion to metal in the range between 823 K and 923 K (550 °C and 650 °C). Therefore, according to the above discussion, despite showing different mechanisms it can be said that a simultaneous hydrogen reduction of NiO and Fe_2O_3 can be considered as a possible method to produce Fe and Ni from a homogeneous mixture of their oxides using pure H_2 as a reducing agent. Moreover, the obtained metals, given sufficient time for atomic diffusion to take place, could then react and form characteristic alloys of the Fe-Ni system, as shown in the phase diagram presented in Figure 3.

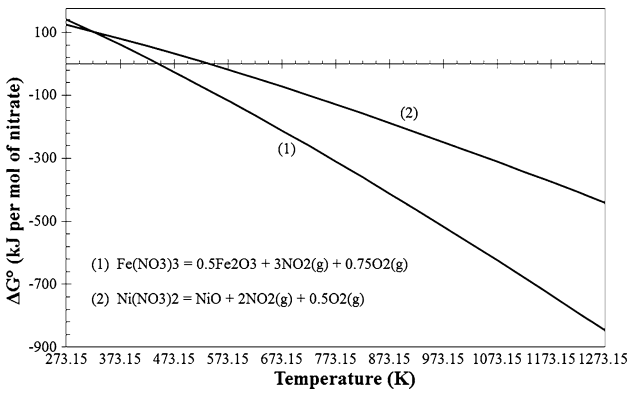

Fig. 1—Standard Gibbs energy for nitrates thermal decomposition.

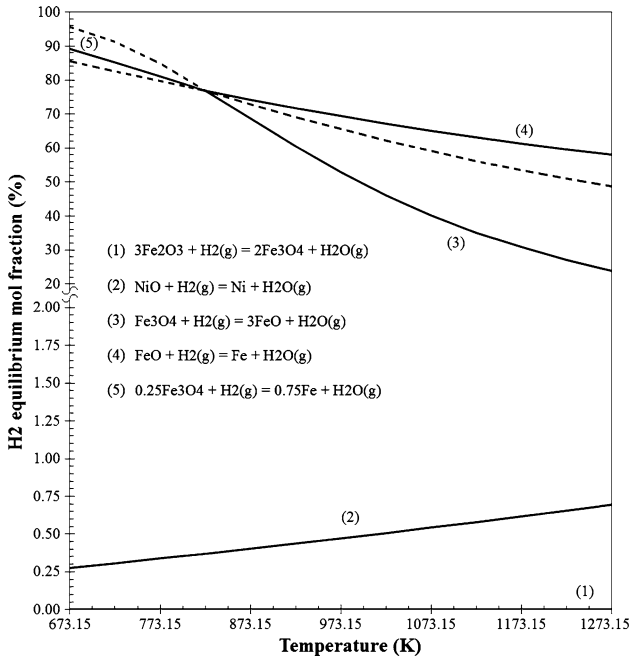

Fig. 2—Hydrogen equilibrium mole fraction as function of the temperature for the iron and nickel oxides reduction.

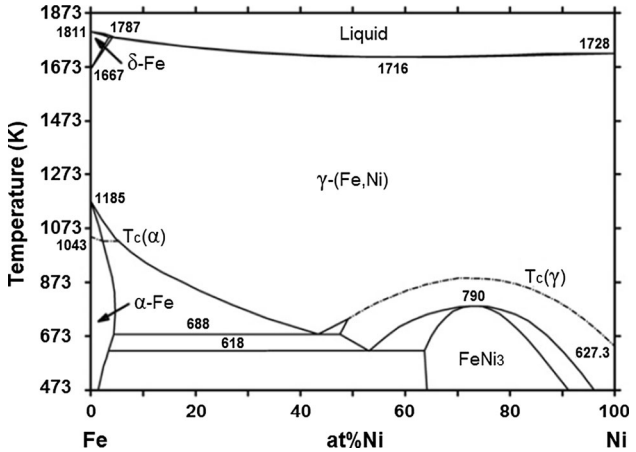

Fig. 3—Fe-Ni phase diagram.[16]

In this context, based on the phase diagram published by Cacciamani *et al.*[16] (Figure 3), the equilibrium cooling of a γ-alloy of FCC structure should result, depending on the initial Fe:Ni ratio, in different mass fractions of alpha (BCC) and $FeNi_3$ (FCC) phases.

Finally, it should be noticed that, during the synthesis experiments conducted in the present study, as hydrogen is admitted into the reduction furnace through a continuous flow, and H_2O continuously removed, chemical equilibrium should be dislocated in the direction of the alloy formation. Thermodynamically speaking, this means that lower reaction temperatures can be implemented. However, the actual conversion as function of time can only be appreciated through kinetic studies.

III. MATERIALS AND METHODS

A. *Experimental Procedure*

In order to obtain iron-nickel alloys with iron mole fractions equal to 20 (A1) and 80 pct (A2), preliminary calculations were made and have established the initial quantities of the respective nitrates necessary for each case. The conditions of temperature and time for thermal decomposition were identified experimentally for both nitrates. Thus, it was found that tests conducted at 623 ± 5 K for 3 hours should result in a full conversion to the desired oxides.

The methodology starts by weighing predetermined amounts of each nitrate ($Fe(NO_3)_3{\cdot}9H_2O$ and $Ni(NO_3)_2{\cdot}6H_2O$) followed by the solubilization in deionized water. The homogeneous aqueous solution is next heated to 623 ± 5 K, and remains at this temperature until all nitrates present decompose resulting in the desired powder oxide mixture, which is then reduced with hydrogen. These tests were performed in a tubular quartz reactor, in which pure commercial H_2 is continuously injected (0.1 L/min), for temperatures equal to 773 K, 823 K, 873 K, and 973 K (500 °C, 550 °C, 600 °C, and 700 °C), and a total reaction time of 60 minutes. It is worthwhile to mention that an analogous methodology has been applied for synthesizing other alloys and composites of technological importance,[13–15] with the possible formation of samples of considerable nanostructured content.

Both iron and nickel oxides containing mixtures (OM1 and OM2) as well as their corresponding Fe-Ni alloys (A1 and A2), were characterized through XRD, for the identification and mass fraction evaluation of the present phases. In relation to the oxide mixtures, microanalysis was also performed through X-ray dispersive energy spectroscopy (EDS) in order to appreciate the global composition of the samples. Finally, after optimizing reduction temperature and time for achieving full conversion to metal, magnetization measurements as a function of the applied external field were accomplished at 300 K (27 °C).

B. *Characterization*

For the XRD analysis and determination of the mean crystallite sizes and mass fractions of phases, an equipment SIEMENS-D5000 was used, which worked in the Bragg–Brentano geometry, Cu source, and graphite monochromator. The XRD data have been analyzed according to the implementation of the Rietveld's method with fundamental parameters, using software TOPAS, version 4.1. On what touches the SEM analysis, an equipment HITASHI TM-3000 was used, which works at 20 kV, backscattered electrons and equipped with an Oxford EDS detector designed for the semi-quantitative determination of elements with atomic number greater than five. The EDS spectra have been analyzed through using software SwiftED3000.

C. *Magnetization Measurements*

The magnetization measurements have been carried out using a GMW bipolar-field electromagnetic system, model 3470.

IV. RESULTS AND DISCUSSION

The experimental results (synthesis and characterization) are presented in the following topics.

A. *Nitrates Thermal Decomposition*

The diffraction patterns obtained by XRD confirmed the exclusive presence of iron and nickel oxides (Fe_2O_3, NiO, and Fe_2NiO_4). Regarding to mixture OM1, the Rietveld analysis of the obtained diffraction data (Figure 4) indicated the presence of Fe_2O_3 and NiO crystals, with mass fractions, respectively, equal to 18.32 and 81.68 pct, and mean crystallite sizes (Fe_2O_3—13.3 nm and NiO—23.1 nm) suggesting a significant nanostructured content.

Moreover, the mass fractions of Ni, Fe, and O (Table I), obtained from EDS microanalysis of the region depicted on Figure 5, are, within the expected experimental error (±5 pct), in accordance with the values obtained from XRD.

In a similar approach, it was observed that mixture OM2 also had a chemical composition consistent with an increased presence of iron (Table II), which was determined through analysis of the EDS spectra associated with the image represented on Figure 6.

The elemental composition of sample OM2 was also confirmed through XRD data analysis (Figure 7), which can be quantitatively described by the presence of Fe_2O_3 and Fe_2NiO_4, with mass fractions, respectively, equal to 45.50 and 55.50 pct. As observed for sample OM1, the calculated mean crystallite sizes (Fe_2O_3—6.3 nm and Fe_2NiO_4—9.2 nm) also suggest a significant nanostructured content. Indeed, the low nitrates decomposition temperatures contribute for the production of oxide particles with low crystallite sizes.[17]

B. *Hydrogen Reduction*

Reduction experiments have been performed at temperatures of 773 K, 823 K, and 873 ± 5 K (500 °C, 550 °C, and 600 ± 5 °C) for different reaction times

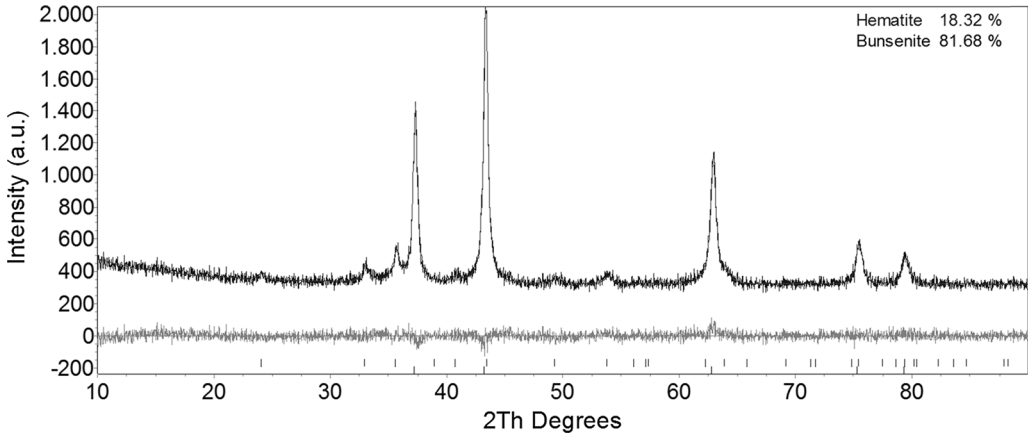

Fig. 4—XRD pattern for oxide mixture OM1.

Table I. Fe, Ni, and O Mass Fractions in OM1 Sample from EDS and XRD Data Analysis

Method	W_{Fe} (pct)	W_{Ni} (pct)	W_O (pct)
XRD	12.8	64.3	23.0
EDS	9.7	69.1	21.3

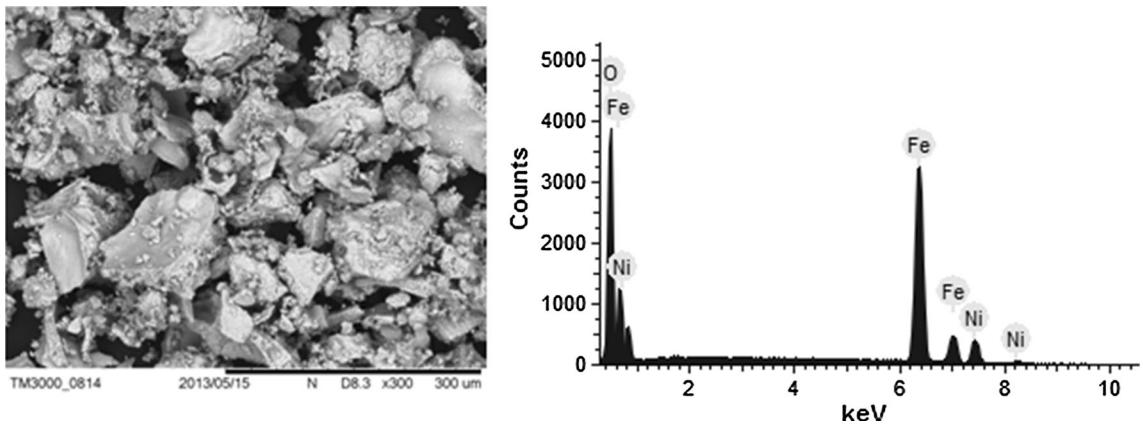

Fig. 5—MEV image and EDS spectra of sample OM1.

Table II. Fe, Ni, and O Mass Fractions in OM2 from EDS and XRD Data Analysis

Method	W_{Fe} (pct)	W_{Ni} (pct)	W_O (pct)
XRD	57.6	13.9	28.5
EDS	61.5	13.1	25.4

(5, 10, 15, 30, 45, and 60 minutes).[18] Figure 8 shows the results for the reduction of the OM1 sample. It can be noticed that the maximum achieved conversion in relation to the total reduction of the two oxides was approximately equal to 97 pct. For OM2 samples, lower conversion levels were observed, with a maximum value of 92 pct (Figure 9). The fact that full reduction could not be achieved for both samples can be explained through re-oxidation and/or the kinetic limitations. The former should be associated with possible contaminations either in the H_2 or in the N_2 used (both commercial grade), and also through reaction with air during weighting. The latter could be explained by the fact that reaction conditions (time and temperature) were, in a first moment, not satisfactorily optimized so as to provide a full conversion to metal.

The decrease in conversion levels for higher iron oxide content is consistent with studies conducted with pure oxide samples,[18] since, for the same reaction time, a complete reduction of Fe_2O_3 requires a significantly higher temperature than for the NiO reaction. Those results are also consistent with the thermodynamics expectations (topic 2.2), which suggest that Fe_2O_3 reduction should develop through multiple reaction steps.

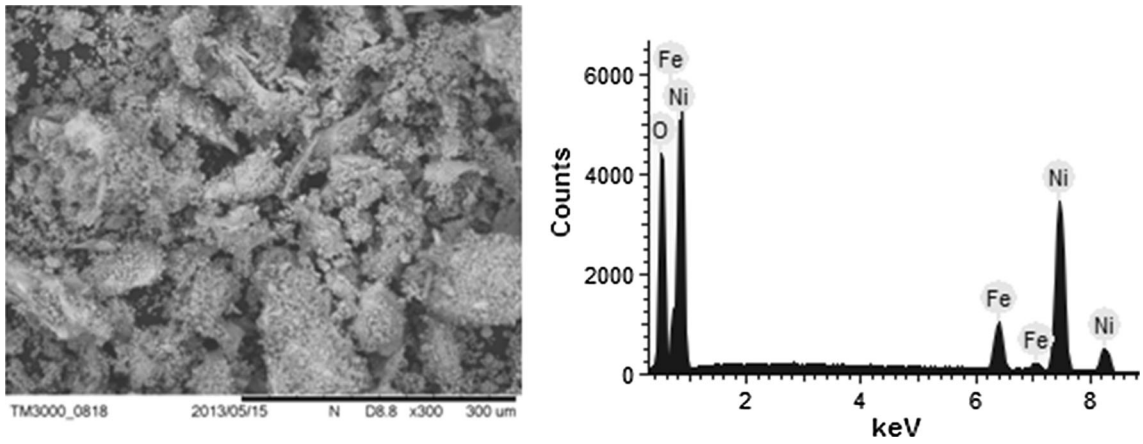

Fig. 6—MEV image and EDS spectra of sample OM2.

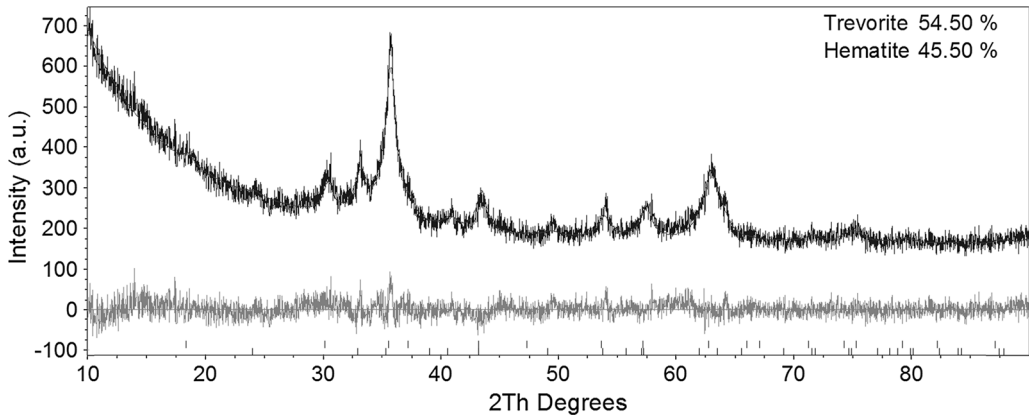

Fig. 7—XRD pattern for oxide mixture OM2.

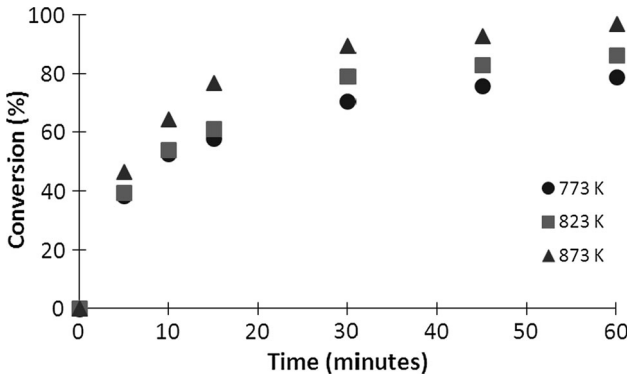

Fig. 8—Reduction conversion as a function of time for sample OM1.

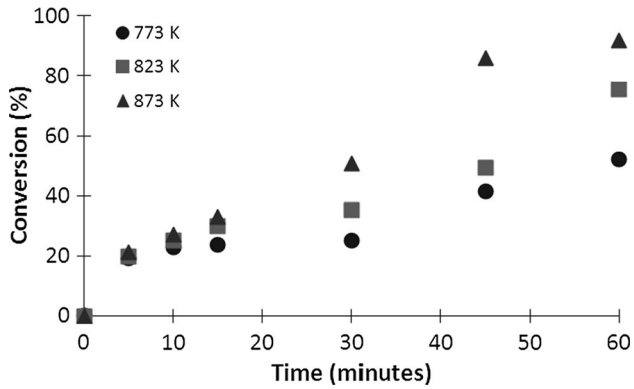

Fig. 9—Reduction conversion as a function of time for sample OM2.

Therefore, in order to achieve full conversion, further tests were carried out at 973 ± 5 K (700 ± 5 °C) for 90 minutes. Also, to minimize re-oxidation, both samples were gradually cooled under N_2 to room temperature. Figures 10(a) and (b) show the XRD patterns obtained for the two synthesized alloys. The position of the diffraction peaks present in the XRD pattern of both samples agree with data from literature for alloys in the Fe-Ni system.[9,19] The alloy phases identified from XRD data agree with the information extracted from the Fe-Ni phase diagram (Figure 3). The higher atomic fraction of iron on sample A2, brings the equilibrium to the region where $FeNi_3$ and alpha should be present in the solid state, whereas for sample A1, only phase $FeNi_3$ is expected.

Moreover, the average crystallite size (26 nm) calculated for each alloy through XRD quantitative analysis suggests that the samples have a significant nanostruc-

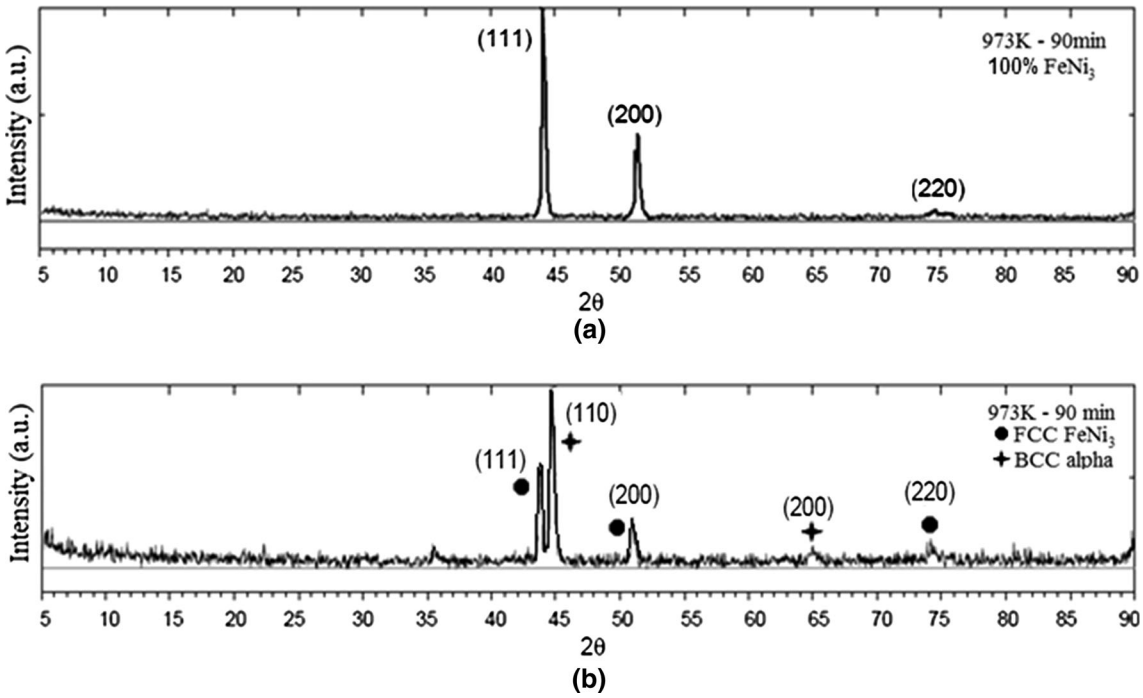

Fig. 10—XRD pattern for reduced samples A1 (*a*) and A2 (*b*).

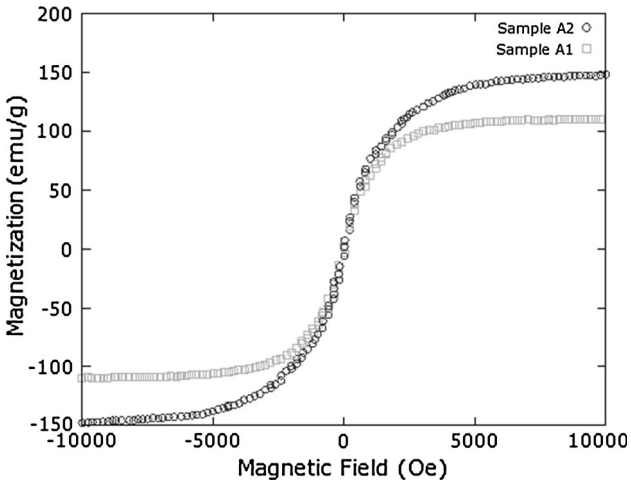

Fig. 11—Specific magnetization of samples A1 and A2 as a function of the applied field.

tured content, a typical result associated with alloys chemical synthesis methods, which are based on the thermal decomposition of a metallic precursors, such as nitrates, for example.[5–9]

C. *Magnetization Measurements*

In order to make a preliminary evaluation of the alloys magnetic behavior, specific magnetization of selected samples has been measured as a function of the applied magnetic field at 300 K (27 °C).[18]

For both samples (A1 and A2), the data suggest a tendency toward superparamagnetism (Figure 11), which is characterized by the absence of a hysteresis loop.[2] The fact that almost no magnetic hysteresis has been detected gives support to the idea that the obtained alloys should contain nanostructured particles, in agreement with the low value found for the calculated mean crystallite size. It is worthwhile to mention that the present saturation magnetization values are similar to the recent published data of Xu *et al.*[5] and Ballot *et al.*[6] The first authors synthesized oxide precursor mixtures containing iron and nickel through thermal treatment of metallic chloride solutions, while the latter employed an alcoholic solution containing iron chloride and nickel acetate. After the thermal decomposition of the prepared solutions, the oxide samples were reduced with H_2 [673 K to 773 K (400 °C to 500 °C)], a very similar methodology in comparison to the one applied in the present work.

V. CONCLUSIONS

According to the proposed methodology, Fe-Ni magnetic nanostructured alloys could be effectively produced. In this context, the presented chemical method can be interpreted as an alternative to other processes already described in the literature for alloy synthesis, such as melting of the individual metals or the formation of the alloy based on the thermal treatment of mechanical mixtures thereof. In the case of the present procedure a homogeneous alloy containing crystals with sizes in the nanometric range could be easily synthesized. The obtained homogeneity is strongly related to the chemical nature of the applied methodology, and the nanometric crystal size mainly determined by the low temperatures involved during the nitrate thermal decomposition [673 K (400 °C)], as well as for the H_2 reduction stage [973 K (700 °C)].

Based on the conversion measurements in different temperatures as a function of time, it was observed that the sample with the highest initial iron content (mixture OM2) reacts slower for the same conditions (temperature and time) in comparison with the sample richer in nickel (mixture OM1). This can be explained based on the mechanism expected for the reduction of each individual metal. In the case of iron, a higher number of reaction steps should be involved (Section II–B), making the process global velocity lower. On the other hand, higher iron content means that the sample has a stronger tendency toward re-oxidation. This again can be explained based on thermodynamic arguments, as iron is more prominent to oxidation in comparison to nickel (Figure 2).

On what touches the nature of the metallic alloys, the results from Rietveld analysis agree with the expectations based on the Fe-Ni phase diagram (Figure 3)—sample A1 (only $FeNi_3$), sample A2 (alpha and $FeNi_3$, with a higher mass fraction of alpha). During the same analysis, the mean crystallite size for the two samples has the same order of magnitude (26 nm), suggesting that both materials should contain a significant amount of nanostructured phases. This idea is indeed in accordance with specific magnetization data (Figure 11), indicating that both samples should behave superparamagnetically.

ACKNOWLEDGMENTS

The authors are grateful to CNPq, FAPERJ, and CAPES for the financial support and scholarships.

REFERENCES

1. G. Herzer: *IEEE Trans. Magn.*, 1989, vol. 25, pp. 3327 29.
2. C.P. Bean and J.D. Livingston: *J. Appl. Phys.*, 1959, vol. 30 (4), pp. 120–29.
3. R.P. Cowburn: *J. Appl. Phys.*, 2003, vol. 93 (11), pp. 9310–15.
4. T. Yokoyama and K. Eguchi: *Phys. Rev. Lett.*, 2011, vol. 107 (6), pp. 065901-1–065901-4.
5. N. Ballot, F. Schoenstein, S. Mercone, T. Chauveau, O. Brinza, and N. Jouini: *J. Alloys Compd.*, 2012, vol. 536, pp. 381–85.
6. M.H. Xu, W. Zhong, X.S. Qi, C.T. Au, Y. Deng, and Y.W. Du: *J. Alloys Compd.*, 2010, vol. 495, pp. 200 04.
7. M. Bahgat, M.K. Paek, and J.J. Pak: *J. Alloys Compd.*, 2008, vol. 466, pp. 59 66 .
8. D.H. Riu and S.T. Oh: *Curr. Appl. Phys.*, 2012, vol. 12, pp. 188–91.
9. H.Q. Wu, Y.J. Cao, P.S. Yuan, H.Y. Xu, and X.W. Wei: *Chem. Phys. Lett.*, 2005, vol. 406, pp. 148–53.
10. S.W. Du and R.V. Ramanujan: *J. Magn. Magn. Mater.*, 2005, vol. 292, pp. 286–98.
11. L.H. Zhu, X.M. Ma, and L. Zhao: *J. Mater. Sci.*, 2001, vol. 36 (23), pp. 5571–74.
12. Y. Liu, J. Zhang, L. Yu, G. Jia, C. Jing, and S. Cao: *J. Magn. Magn. Mater.*, 2005, vol. 285, pp. 138–44.
13. E.A. Brocchi, M.S. Motta, and P.K. Jena: *Metall. Mater. Trans. B*, 2004, vol. 35B, pp. 1107–12.
14. P.K. Jena, E.A. Brocchi, and M.S. Motta: *Mater. Sci. Eng. A*, 2001, vol. 313, pp. 180–86.
15. E.A. Brocchi, M.S. Motta, I.G. Solórzano, P.K. Jena, and F.J. Moura: *Mater. Sci. Eng. B*, 2004, vol. 112 (2–3), pp. 200–05.
16. G. Cacciamani, J. De Keyzer, R. Ferro, U.E. Klotz, J. Lacaze, and P. Wollants: *Intermetallics*, 2006, vol. 14, pp. 1312–25.
17. E.A. Brocchi, R.C.S. Navarro, M.S. Motta, F.J. Moura, and I.G. Solórzano: *Mater. Chem. Phys.*, 2013, vol. 140, pp. 273–83.
18. O.A. Cortez: Doctorate Thesis, Materials Engineering Department, Catholic University of Rio de Janeiro, Rio de Janeiro, Brazil, 2008.
19. A. Lutts and P.M. Gielen: *Phys. Status Solidi*, 1970, vol. 41, pp. 81–84.